Available online at www.sciencedirect.com

ScienceDirect

Mendeleev Commun., 2022, **32**, 527–530

Mendeleev Communications

Synthesis and photovoltaic properties of novel (X-DADAD)$_n$ conjugated polymers with fluorene and phenylene blocks

Ilya E. Kuznetsov,*[a] Maxim E. Sideltsev,[a] Vladimir G. Kurbatov,[a] Mikhail V. Klyuev[b] and Alexander V. Akkuratov[a]

[a] *Institute of Problems of Chemical Physics, Russian Academy of Sciences, 142432 Chernogolovka, Moscow Region, Russian Federation. E-mail: kusnetsovilja@gmail.com*
[b] *Ivanovo State University, 153025 Ivanovo, Russian Federation*

DOI: 10.1016/j.mencom.2022.07.031

Novel fluorene- and phenylene-based conjugated polymers with the TBTBT molecular framework consisting of the thiophene (T) and benzothiadiazole (B) building blocks have been synthesized and investigated. It has been demonstrated that the variation of X building blocks with branched side chains in (X-TBTBT)$_n$-type structures, as well as the introduction of fluorine into the main chain, strongly affects the optical, electronic and physicochemical properties of the obtained polymers. The phenylene-based polymer with a fluorine-loaded TBTBT block achieves a power conversion efficiency of 7% in organic solar cells, which can be further improved by optimizing the active layer morphology.

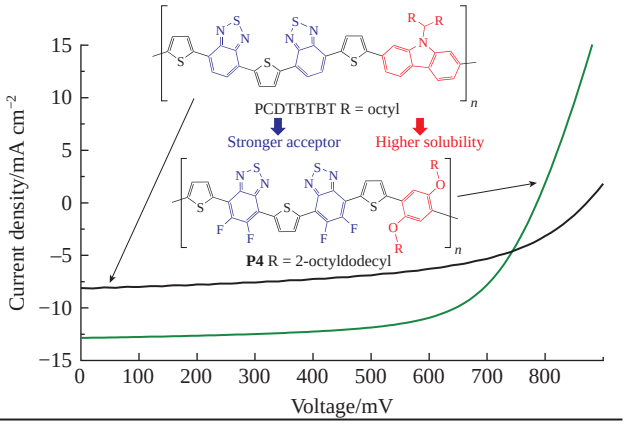

Keywords: benzothiadiazole, thiophene, branched side chains, conjugated polymer, organic solar cells.

Conjugated polymers are promising semiconductor materials for organic photovoltaic devices based on p–n junction. Among them, organic solar cells (OSCs),[1,2] organic light-emitting diodes[3] and organic photodetectors[4] have received considerable attention in recent years due to their important advantages over inorganic analogues, such as flexibility, light weight, stretchability[5] and semitransparency.[6] Furthermore, organic photovoltaic devices can be fabricated over large areas using low-cost, high-throughput printing technologies.[7]

High-performance conjugated polymers are usually designed based on the push-pull concept, in which the polymer backbone consists of alternating electron donor (D) and electron acceptor (A) building blocks bearing different substituents. This makes it possible to tune the optical and electronic properties of these materials, as well as their charge-transport characteristics and solubility in organic solvents.[8,9] Most of the conjugated polymers developed for OSCs have the (X-DAD)$_n$ molecular structure, where X is the various polycyclic aromatic or heteroaromatic units such as carbazole, fluorene and benzodithiophene. We recently proposed an alternative approach to design conjugated polymers containing an extended DADAD molecular motif instead of DAD systems.[10] The (X-DADAD)$_n$ polymers exhibited improved optoelectronic properties compared to the (X-DAD)$_n$ analogues. In particular, the carbazole-containing polymer PCDTBTBT has a narrower band gap (E_g = 1.7 eV) than its well-known (X-DAD)-type counterpart PCDTBT (E_g = 1.9 eV).[11] The decrease in the PCDTBTBT band gap energy is associated with a decrease in the energy of the lowest unoccupied molecular orbital (LUMO) upon the introduction of an additional electron-deficient benzothiadiazole (B) unit, while the energy of the highest occupied molecular orbital (HOMO) remains almost the same (*ca.* −5.5 eV). Thus, according to the Sharber models,[12] PCDTBTBT could provide improved OSC photovoltaic performance in terms of short circuit current density and open circuit voltage. However, the extremely low solubility of PCDTBTBT prevented the expected power conversion efficiency (PCE) of practical devices from being achieved.[9] We recently reported an approach to improve the solubility of PCDTBTBT by replacing terminal thiophene fragments with alkylthienyl moieties[9] or by using X-blocks with solubilizing bulky alkyl substituents.[13] Unfortunately, OSCs based on the obtained polymers exhibited poor PCEs.

In this work, we designed three novel (X-DADAD)$_n$ conjugated polymers that include fluorene and phenylene structural X-blocks bearing long-chain 2-octyldodecyl substituents and TBTBT blocks (T is a thiophene donor block, B is benzothiadiazole or 5,6-difluorobenzothiadiazole acceptor block) along with unsubstituted thiophene rings. The introduction of two branched alkyl chains into fluorene or phenylene moieties ensures good solubility of polymers and avoids undesirable steric effects. OSC based on phenylene-containing polymer **P4** demonstrated a PCE of 7.0%, which is remarkably higher than the efficiency of PCDTBTBT-based devices, and indicates the great potential of the proposed approach for the design of semiconductor (X-DADAD)$_n$ polymers.

Scheme 1 shows the synthesis of conjugated polymers **P1**–**P4**. All polymers were synthesized by the palladium-catalyzed Stille polycondensation reaction using monomers **1**–**4** prepared according to previously reported procedures.[14] The crude polymers were fractionated in a Soxhlet apparatus by sequential extraction with acetone, dichloromethane and finally chlorobenzene. The chlorobenzene fractions of the polymers were collected, concentrated and poured into ethanol. The precipitated polymers were filtered and dried in vacuum.

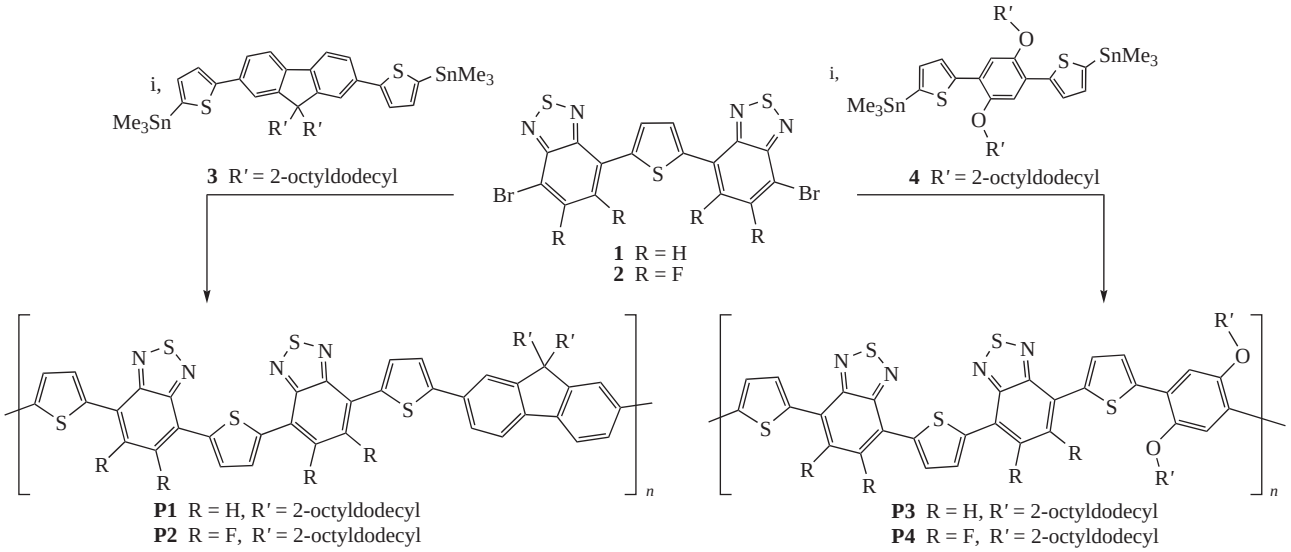

Scheme 1 *Reagents and conditions*: i, $Pd_2(dba)_3$, (*o*-Tol)$_3$P, toluene, reflux.

Table 1 Physicochemical, optical and electrochemical properties of polymers **P1**–**P4**.

Polymer	M_w/kDa	M_w/M_n	T_d/°C	λ_{max}^{sol}/nm	λ_{max}^{film}/nm	E_g/eV	E_{onset}^{ox} (*vs.* Fc^+/Fc)/V	HOMO/eV	LUMO/eV
P1	44	1.7	405	539	596	1.77	0.66	−5.76	−3.99
P2	53	1.3	405	528	602	1.88	0.90	−6.00	−4.12
P3	32	1.2	405	545	668	1.61	0.28	−5.38	−3.77
P4	24	1.5	380	535	598	1.72	0.50	−5.60	−3.88

We investigated the molecular weight characteristics of the synthesized polymers by gel permeation chromatography as described previously[15] and obtained weight-average molecular weights in the range of 24–53 kDa and polydispersity indices (M_w/M_n) of 1.2–1.7 (Table 1).

The optical properties of the polymers were investigated in a solution of 1,2-dichlorobenzene and in thin films [Figure 1(*a*),(*b*)]. The absorption bands at shorter wavelengths (350–470 nm) correspond to the π–π* transition in the polymers, while the band at longer wavelengths (500–750 nm) can be associated with intramolecular charge transfer.

Polymer **P4** exhibits a shoulder peak at about 600 nm, suggesting aggregation of polymer molecules in dilute solution at room temperature. In the case of thin films, a strong bathochromic shift of the absorption bands by 70–120 nm is observed (Table 1). This indicates efficient self-assembly of macromolecules in the solid state. The optical band gap (E_g^{opt}) of polymers **P1**–**P4** was estimated from Tauc plots for the spectra of thin films [Figure 1(*c*) and Table 1].[16]

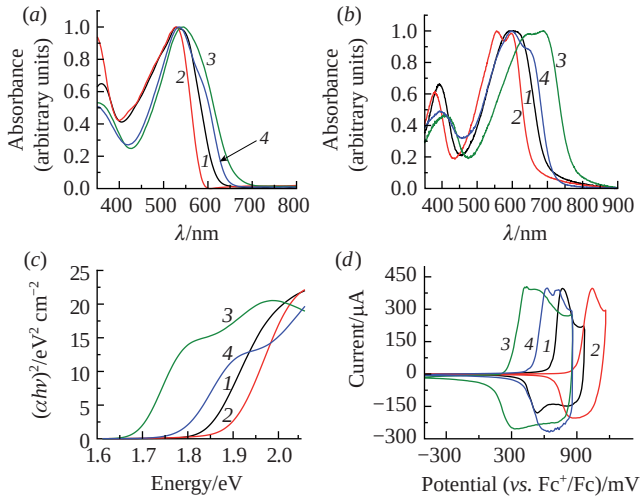

Figure 1 Absorption spectra (*a*) in solution and (*b*) in thin films, (*c*) Tauc plots and (*d*) cyclic voltammograms of (*1*) polymer **P1**, (*2*) polymer **P2**, (*3*) polymer **P3** and (*4*) polymer **P4**.

Conjugated polymers **P3** and **P4** containing phenylene blocks have a smaller band gap compared to fluorene-containing compounds **P1** and **P2**. The observed differences may be related to the electronic structure of block X and steric effects. In particular, electron-donating alkoxy groups significantly increase the HOMO energy of polymers **P3** and **P4**, thus reducing their band gap.[17,18] Furthermore, non-covalent interactions between the H atoms of thiophene and the O atoms of the alkoxy groups minimize dihedral angles, thereby increasing the planarity of the polymer chain and the effective length of the π-system, which leads to a decrease in the band gap.[19] On the contrary, bulky alkyl chains on the sp^3 carbon atoms of the fluorene units can distort the planar structure of the polymer backbone.[20] As a result, the band gap of these polymers is larger than that of polymers **P3** and **P4**. It should be noted that fluorine-containing polymers **P2** and **P4** have a wider band gap, which may be due to the effect of fluorine on the energy of the frontier orbitals of the polymers.[21]

The electrochemical properties of the polymers were investigated by cyclic voltammetry. The recorded cyclic voltammograms are shown in Figure 1(*d*). Onset oxidation potentials (E_{onset}^{ox}) were measured against the Ag/Ag^+ reference electrode using a ferrocenium/ferrocene (Fc^+/Fc) redox couple with an absolute energy of −5.10 eV relative to a vacuum as an internal standard (see Table 1).[22] The LUMO levels were calculated based on the estimated HOMO energies and optical band gaps of the respective polymers.

The HOMO energies of polymers P3 and P4 turned out to be 0.4–0.5 eV higher than those of fluorene-containing polymers. The introduction of fluorine into the backbones of polymers **P2** and **P4** led to a decrease in the HOMO energy by ~0.23 eV. These observations are consistent with previously published results.[23]

As can be seen, the conjugated polymer **P2** has an extremely low HOMO energy (−6.0 eV), comparable to that of fullerene derivatives [60]PCBM and [70]PCBM.[24,25] On the one hand, this

Table 2 Parameters of OSCs based on blends of polymers **P1**–**P4** with [70]PCBM.

Polymer	Processing conditions			V_{OC}/ mV	J_{SC}/ mA cm^{-2}	FF (%)	η (%)	μ_e/ cm^2 V^{-1} s^{-1}	μ_h/ cm^2 V^{-1} s^{-1}	μ_e/μ_h
	Polymer/[70]PCBM weight ratio	Composite film thickness/nm	Total concentration of polymer + [70]PCBM /mg cm^{-3}							
P1	1 : 2.0	120	18	905	8.1	57	4.2	3.3×10^{-6}	2.2×10^{-6}	1.50
P2	1 : 2.5	140	28	920	6.8	29	1.8	4.2×10^{-6}	8.6×10^{-5}	0.05
P3	1 : 2.0	160	18	631	10.1	65	4.2	5.3×10^{-4}	3.9×10^{-4}	1.36
P4	1 : 1.5	135	15	786	13.0	69	7.0	1.4×10^{-3}	2.5×10^{-3}	0.56

polymer can provide a high open-circuit voltage of OSCs, since this parameter correlates with the energy gap between the HOMO of the donor and the LUMO of the acceptor materials.[26] On the other hand, a narrow gap between the donor and acceptor frontier orbitals can hinder the effective dissociation of excitons, worsening the OSC parameters. It can be noted that the high-lying energy level of the HOMO of polymer **P3** will limit the open-circuit voltage of OSCs.

Thus, an analysis of the optoelectronic properties of the polymers revealed that polymers **P1** and **P2** can provide high open-circuit voltages, and polymers **P3** and **P4** can provide high short-circuit currents in OSCs. At the same time, polymer **P2** can be used as an acceptor component in all-polymer solar cells.

Thermal properties of the polymers were investigated by thermal gravimetric analysis and differential scanning calorimetry (DSC). All polymers exhibited high thermal stability.† Decomposition temperatures of the polymers are more than 350 °C, which makes it possible to use them for the manufacture of OSCs. There are no obvious peaks of phase transitions on the DSC curves, which indicates the amorphous nature of all polymers.†

The obtained polymers were investigated as donor materials in OSCs with standard configuration: ITO/PEDOT:PSS/polymer–fullerene composite/Mg/Al. The fullerene derivative [70]PCBM was used as an electron acceptor.[24] The *J*–*V* characteristics of the solar cells [Figure 2(*a*)] were measured under one sun illumination provided by a KHS Steuernagel solar simulator (AM1.5G, 100 mW cm^{-2}). In order to improve the performance of the devices, the conditions for their manufacture were optimized. The acceptor component, the donor/acceptor ratio in the blend, the thickness of the active layer and the post-treatment of the blend films were varied. The parameters of optimized devices are presented in Table 2.

OSCs demonstrated PCE ranging from 1.8% to 7.0%. The highest PCE of 7% was provided by polymer **P4** containing phenylene moieties and difluorobenzothiadiazole blocks, while its non-fluorinated analogue **P3** showed a lower efficiency of 4.2%.

Despite the band gap that is smaller than that of polymer **P3**, polymer **P4** provides the highest photocurrent of 13 mA cm^{-2} in OSCs. This value is well confirmed by the external quantum efficiency (EQE) spectra. The maximum in the EQE spectrum for the composite based on polymer **P4** reaches ~75% [Figure 2(*b*), curve *4*]. The difference in the current densities of the devices can be explained by the different charge-transport characteristics of polymer–fullerene blend films. Measurements of the charge carrier mobility using the space charge limited current technique[27] showed that the values of μ_e and μ_h for films of blends based on polymer **P4** are 2–3 orders of magnitude higher than those for films of other composites (see Table 2).† At the same time, the introduction of fluorine atoms into polymer **P2** did not lead to an improvement in the J_{SC} values of corresponding devices. Moreover, OSCs based on polymer **P2** exhibited the lowest fill factors (FFs). The zero gap between the LUMO (−6.0 eV) and HOMO (−4.2 eV) of PCBM[28] and the LUMO and HOMO of polymer **P2**, respectively, is responsible for poor charge separation and low levels of J_{SC} and FF in OSCs. The maximum values of the open-circuit voltages of 920 mV in the devices are associated with the low-lying energy level of the HOMO of polymer **P2**, as we mentioned above.

We also examined the surface of the blend films using atomic force microscopy (AFM). The AFM images are presented in Figure 3. Root-mean-square (RMS) roughness of films of polymers **P1**–**P3** is *ca.* 0.6–1.0 nm. The average cluster size is in the range of 30–80 nm, which is favorable for the generation and dissociation of excitons, as well as the further transport of charge carriers to the electrodes.[29,30] Thus, the parameters of optimized solar cells are affected by the electrophysical and optoelectronic properties of conjugated polymers.

It should be noted that the **P4**/[70]PCBM system providing the maximum PCE in OSCs has a higher RMS value of ~3 nm,

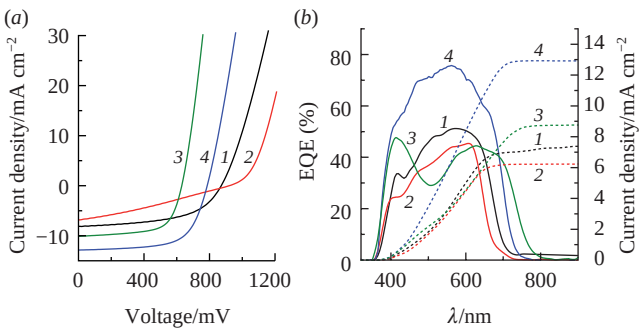

Figure 2 (*a*) *J*–*V* characteristics and (*b*) EQE spectra of optimized solar cells based on blends of (*1*) polymer **P1**, (*2*) polymer **P2**, (3) polymer **P3** and (*4*) polymer **P4** with [70]PCBM.

† For details, see Online Supplementary Materials.

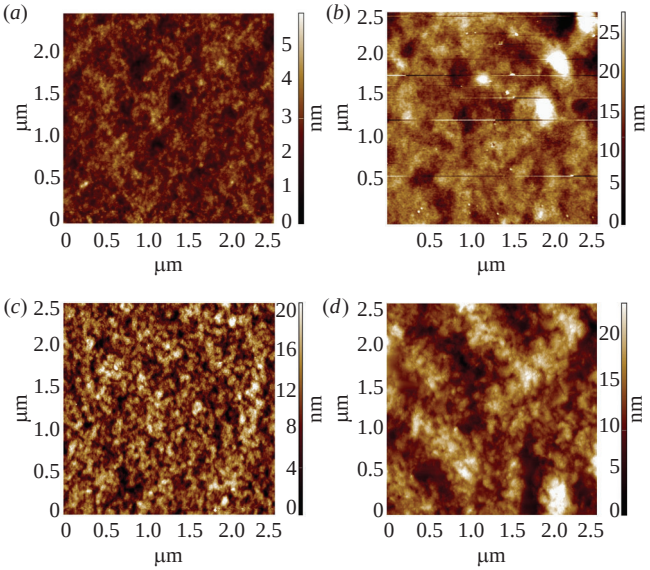

Figure 3 AFM images of films made from blends of (*a*) polymer **P1**, (*b*) polymer **P2**, (*c*) polymer **P3** and (*d*) polymer **P4** with [70]PCBM. The RMS roughness and average cluster size of these films are 0.2, 0.91, 1.05 and 2.89 nm and 35, 81, 30 and 50 nm, respectively.

which can be explained by the lower miscibility of the polymer with the fullerene derivative. This result allows us to expect a significant increase in the efficiency of solar cells when optimizing the conditions for preparing the composite film.

In conclusion, three novel conjugated polymers of the $(X\text{-DADAD})_n$ type were synthesized. The combination of phenylene moieties bearing long-chain 2-octyldodecyl substituents with a fluorine-loaded TBTBT molecular framework provided optimal optoelectronic and physicochemical properties of polymer **P4**. As a result, OSC based on the **P4**/[70]PCBM system exhibited a PCE of 7%. There is great scope for improving the performance of OSCs by optimizing the morphology of **P4** polymer blend films as well as the use of modern non-fullerene acceptors.

This work was supported by the Russian Foundation for Basic Research (project no. 20-03-00309) and the Ministry of Science and Higher Education of the Russian Federation (project no. AAAA-A19-119101590029-0). We acknowledge the participation of Dr. P. M. Kuznetsov in the characterization of OSCs. The authors also gratefully thank Dr. P. A. Troshin for access to the equipment of the FMEM laboratory at IPCP RAS. The work was performed using the equipment of the Multi-User Analytical Center at IPCP RAS.

Online Supplementary Materials

Supplementary data associated with this article can be found in the online version at doi: 10.1016/j.mencom.2022.07.031.

References

1 Y. Xu, J. Yuan, S. Zhou, M. Seifrid, L. Ying, B. Li, F. Huang, G. C. Bazan and W. Ma, *Adv. Funct. Mater.*, 2019, **29**, 1806747.
2 M. L. Keshtov, S. A. Kuklin, I. O. Konstantinov, Y. Zou and G. D. Sharma, *Mendeleev Commun.*, 2021, **31**, 800.
3 D. Han, Y. Khan, J. Ting, S. M. King, N. Yaacobi-Gross, M. J. Humphries, C. J. Newsome and A. C. Arias, *Adv. Mater.*, 2017, **29**, 1606206.
4 X. Xu, X. Zhou, K. Zhou, Y. Xia, W. Ma and O. Inganäs, *Adv. Funct. Mater.*, 2018, **28**, 1805570.
5 T. Higashihara, *Polym. J.*, 2021, **53**, 1061.
6 Y. Xia, X. Xu, L. E. Aguirre and O. Inganäs, *J. Mater. Chem. A*, 2018, **6**, 21186.
7 J. S. Chang, A. F. Facchetti and R. Reuss, *IEEE Journal on Emerging and Selected Topics* in *Circuits and Systems*, 2017, **7**, 7.
8 O. O. Adegoke, I. H. Jung, M. Orr, L. Yu and T. Goodson, III, *J. Am. Chem. Soc.*, 2015, **137**, 5759.
9 J.-H. Dou, Y.-Q. Zheng, T. Lei, S.-D. Zhang, Z. Wang, W.-B. Zhang, J.-Y. Wang and J. Pei, *Adv. Funct. Mater.*, 2014, **24**, 6270.
10 A. V. Akkuratov, D. K. Susarova, O. V. Kozlov, A. V. Chernyak, Y. L. Moskvin, L. A. Frolova, M. S. Pshenichnikov and P. A. Troshin, *Macromolecules*, 2015, **48**, 2013.
11 A. V. Akkuratov, D. K. Susarova, O. A. Mukhacheva and P. A. Troshin, *Mendeleev Commun.*, 2016, **26**, 248.
12 M. C. Scharber, *Adv. Mater.*, 2016, **28**, 1994.
13 I. E. Kuznetsov, P. M. Kuznetsov, M. I. Ustinova, K. E. Zakirov, P. A. Troshin and A. V. Akkuratov, *Phys. Status Solidi A*, 2021, **218**, 2000816.
14 I. E. Kuznetsov, P. M. Kuznetsov, A. V. Maskaev, A. V. Akkuratov and P. A. Troshin, *Mendeleev Commun.*, 2020, **30**, 683.
15 A. V. Akkuratov, F. A. Prudnov, L. N. Inasaridze and P. A. Troshin, *Tetrahedron Lett.*, 2017, **58**, 97.
16 P. Makuła, M. Pacia and W. Macyk, *J. Phys. Chem. Lett.*, 2018, **9**, 6814.
17 Z. Liu, Y. Hu, P. Li, J. Wen, J. He and X. Gao, *J. Mater. Chem. C*, 2020, **8**, 10859.
18 D. Hashemi, X. Ma, R. Ansari, J. Kim and J. Kieffer, *Phys. Chem. Chem. Phys.*, 2019, **21**, 789.
19 T. L. Nguyen, H. Choi, S.-J. Ko, M. A. Uddin, B. Walker, S. Yum, J.-E. Jeong, M. H. Yun, T. J. Shin, S. Hwang, J. Y. Kim and H. Y. Woo, *Energy Environ. Sci.*, 2014, **7**, 3040.
20 C.-H. Lee, Y.-Y. Lai, J.-Y. Hsu, P.-K. Huang and Y.-J. Cheng, *Chem. Sci.*, 2017, **8**, 2942.
21 S.-J. Ko, Q. V. Hoang, C. E. Song, M. A. Uddin, E. Lim, S. Y. Park, B. H. Lee, S. Song, S.-J. Moon, S. Hwang, P.-O. Morin, M. Leclerc, G. M. Su, M. L. Chabinyc, H. Y. Woo, W. S. Shin and J. Y. Kim, *Energy Environ. Sci.*, 2017, **10**, 1443.
22 C. M. Cardona, W. Li, A. E. Kaifer, D. Stockdale and G. C. Bazan, *Adv. Mater.*, 2011, **23**, 2367.
23 N. Leclerc, P. Chávez, O. A. Ibraikulov, T. Heiser and P. Lévêque, *Polymers*, 2016, **8**, 11.
24 J. C. Hummelen, B. W. Knight, F. LePeq, F. Wudl, J. Yao and C. L. Wilkins, *J. Org. Chem.*, 1995, **60**, 532.
25 M. M. Wienk, J. M. Kroon, W. J. H. Verhees, J. Knol, J. C. Hummelen, P. A. van Hal and R. A. J. Janssen, *Angew. Chem.*, 2003, **115**, 3493.
26 C. J. Brabec, A. Cravino, D. Meissner, N. S. Sariciftci, T. Fromherz, M. T. Rispens, L. Sanchez and J. C. Hummelen, *Adv. Funct. Mater.*, 2001, **11**, 374.
27 Y. Xin, G. Zeng, J. OuYang, X. Zhao and X. Yang, *J. Mater. Chem. C*, 2019, **7**, 9513.
28 T. Umeyama, Y. Watanabe, E. Douvogianni and H. Imahori, *J. Phys. Chem. C*, 2013, **117**, 21148.
29 D. E. Markov, C. Tanase, P. W. M. Blom and J. Wildeman, *Phys. Rev. B: Condens. Matter Mater. Phys.*, 2005, **72**, 045217.
30 D. E. Markov, E. Amsterdam, P. W. M. Blom, A. B. Sieval and J. C. Hummelen, *J. Phys. Chem. A*, 2005, **109**, 5266.

Received: 23rd November 2021; Com. 21/6757